Indian Journal of Chemistry
Vol. 51A, Jan-Feb 2012, pp. 32-46

Selective synthesis of metallic and semiconducting single-walled carbon nanotubes

Rakesh Voggu[a], A Govindaraj[a, b] & C N R Rao[a, b, *]

[a]CSIR Centre of Excellence in Chemistry, Chemistry and Physics of Materials Unit, and International Centre for Materials Science, Jawaharlal Nehru Centre for Advanced Scientific Research, Jakkur P O, Bangalore 560 064, India
[b]Solid State and Structural Chemistry Unit, Indian Institute of Science, Bangalore 560 012, India
Email: cnrrao@jncasr.ac.in.

Received 12 November 2011

As-prepared single-walled carbon nanotubes (SWNTs) are generally mixtures of semiconducting and metallic species, the proportion of the former being around 67%. Since most applications of SWNTs are best served by semiconducting or metallic nanotubes, rather than by mixtures of the two, methods which would directly yield semiconducting and metallic SWNTs in pure form are desirable. In this article, we present the available methods for the direct synthesis of such SWNTs along with the methods available to separate semiconducting and metallic SWNTs from mixtures. We also discuss the synthesis of Y-junction carbon nanotubes.

Keywords: Carbon nanotubes, Nanocarbons, Selective synthesis, Y-junction, Semiconducting SWNT, Metallic SWNT

Carbon nanomaterials constitute a topic of prime research interest today. There are three forms of nanocarbons, namely, fullerenes, carbon nanotubes and graphene. Although graphene has become the flavor of the day in recent years, carbon nanotubes continue to be materials with immense potential for applications. Carbon nanotubes are characterized by a chiral vector, $\mathbf{C}_h = n\vec{a}_1 + m\vec{a}_2$, where n and m are indices that define the nature of the nanotubes[1-3] (Fig. 1). Single-walled carbon nanotubes (SWNTs) can either be semiconducting or metallic depending on the (n, m) values. They are metallic when |n-m| = 3j, where j is an integer. Various methods have been developed for the synthesis of SWNTs and a majority of the methods involving arc-discharge, laser irradiation or chemical vapor deposition yield polydisperse samples with different chiral indices[1]. Generally, as-synthesized SWNTs contain 66% of semiconducting species and 33% of metallic species. Metallic and semiconducting SWNTs can be readily distinguished from their unique signatures in Raman as well as electronic spectra[1]. There have been several attempts to produce SWNTs with well-defined chirality and electronic structure. There is also some progress in the preparation of SWNTs enriched in either the semiconducting or the metallic species at the synthesis level[3-10] or through post-synthetic procedures[11-17]. In this article, we present recent developments in the selective synthesis of metallic and semiconducting SWNTs and the separation strategies devised to attain either type of SWNTs in pure form. We also briefly discuss the synthesis of Y-junction carbon nanotubes.

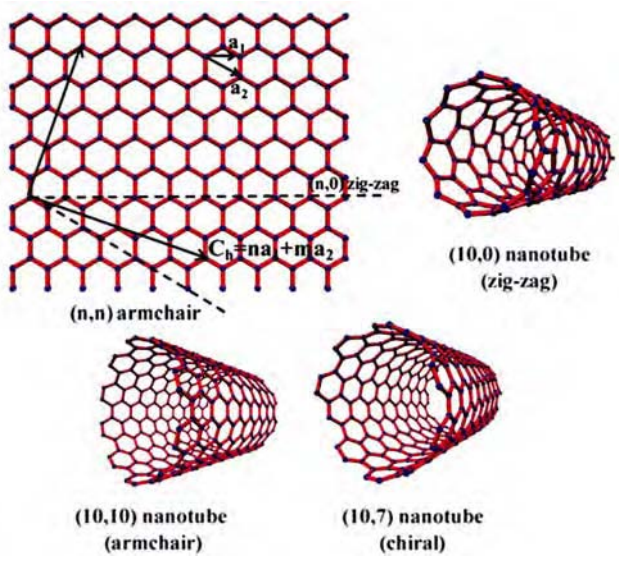

Fig. 1 — Schematic representation of the relation between nanotubes and graphene. $\mathbf{C}_h = n\vec{a}_1 + m\vec{a}_2$ is a graphene 2D lattice vector, where a_1 and a_2 are unit vectors. Integers n and m uniquely define the tube diameter, chirality and metal vs semiconducting nature. [Reproduced from Ref. 3 with permission from Royal Society of Chemistry, London, UK].

Characterization of Metallic and Semiconducting SWNTs

Raman and optical spectroscopies are important tools to characterize SWNTs. The Raman band of SWNTs centered around 1580 cm^{-1} (G-band) exhibits a feature at 1540 cm^{-1}, characteristic of metallic SWNTs. The G-band can be deconvoluted to get the relative proportions of metallic and semiconducting species. The radial breathing mode (RBM) in the Raman spectra of SWNTs is useful for determining the diameter and the (n, m) values of nanotubes (Fig. 2)[18,19]. The RBM frequency is inversely related to the tube diameter.

All the optical spectroscopic features of semiconducting SWNTs and most in metallic SWNTs are attributed to transitions between van-Hove singularities. The presence of energy gaps is induced by features such as doping, curvature and bundling. A small energy gap at the Fermi level opens up in the case of metallic nanotubes due to the curvature of the graphene sheet[20]. Typical optical absorption spectra of SWNTs are shown in Fig. 3(a)[21]. The near-infrared

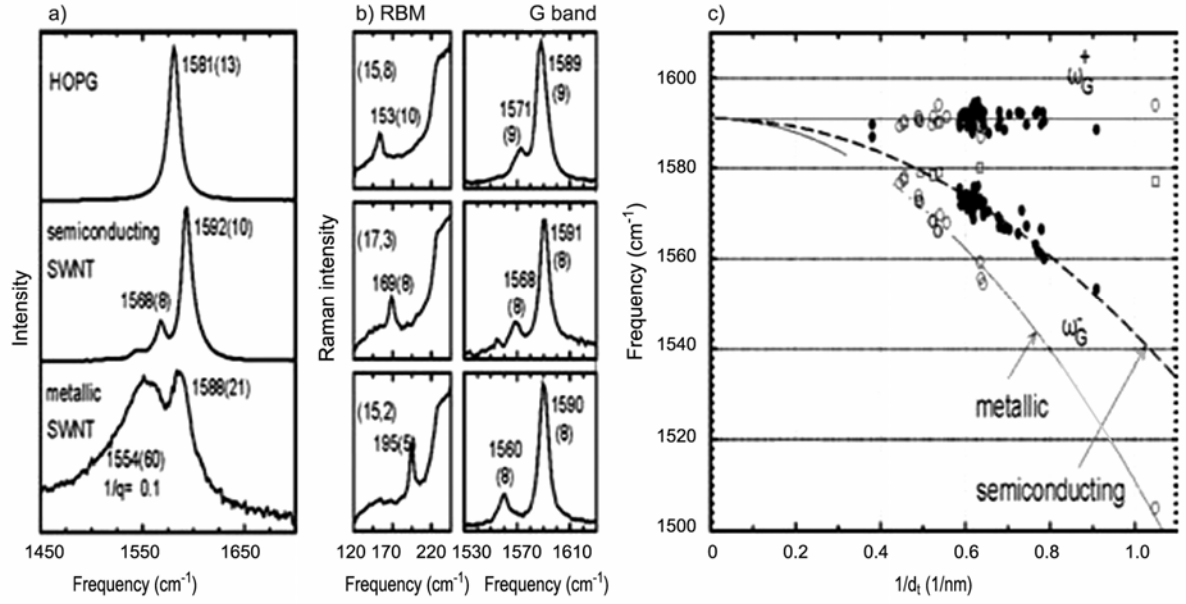

Fig. 2 — (a) Raman G-band of highly oriented pyrolytic graphite (HOPG), a semiconducting SWNT and a metallic SWNT. (b) RBM and G-band bands of three isolated semiconducting SWNTs with the (n,m) values. (c) Frequency versus $1/d_\tau$ for the two most intense G-band (ω_{G-} and ω_{G+}) for isolated SWNTs. [Reproduced from Ref. 18 with permission from American Chemical Society, Washington DC, USA and Ref. 19 from Elsevier, Amsterdam, Netherlands].

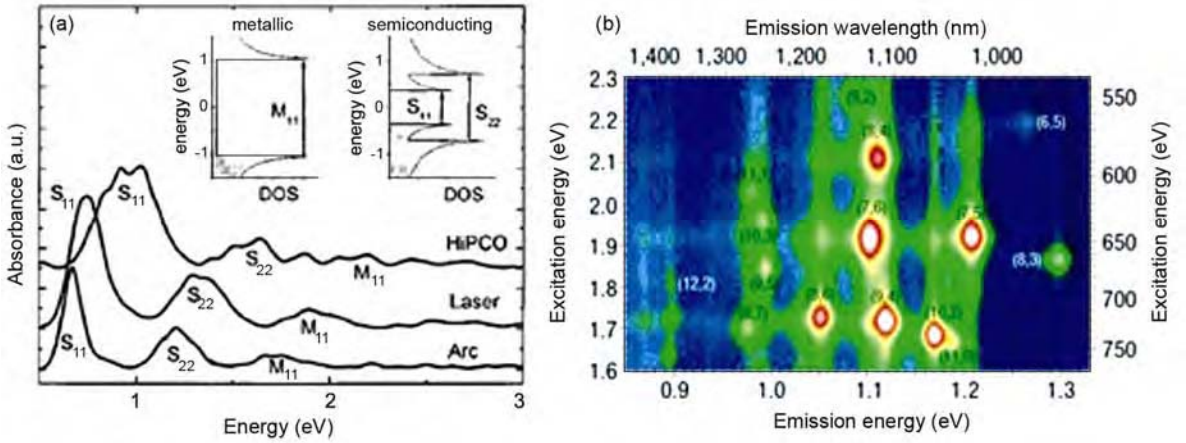

Fig. 3 — (a) Optical absorption spectra of films of purified SWNTs. Here S and M stand for electronic transitions of semiconducting and metallic SWNTs respectively. (b) 2D photoluminescence map of HiPco SWNTs. [Reproduced from Ref. 21 with permission from American Chemical Society, Washington DC, USA].

transitions designated at S_{11} and S_{22} arise from the inter-van Hove energy levels in semiconducting SWNTs, while metallic SWNTs exhibit M_{11} absorption bands in the visible region. Metallic SWNTs show a band (M_{00}) in the infrared spectrum (100 cm^{-1}) due to the small gap near the Fermi level (attributed to effects of finite curvature and broken symmetry). The absorption spectra of SWNTs show a blue shift as the diameter of the nanotube decreases.

Bundled SWNTs do not exhibit photoluminescence as the electron-hole pair non-radiatively decay due to the presence of metallic SWNTs in the bundles. Photoluminescence is observed when the nanotubes are individualized, the process occuring in three steps: (a) an absorption of light at S_{22} followed by (b) a relaxation from S_{11} using a phonon-electron interaction, and, (c) a spontaneous emission at E_{11}. As the energy of the van-Hove singularities maxima are mainly dependent on the nanotube chirality, the (n,m) values of the different nanotubes present in a sample can be characterized using two-dimensional photoluminescence mapping. A typical photoluminescence map of HiPco SWNTs is shown in Fig. 3(b).

Synthesis of Semiconducting SWNTs

Developing methods for the direct synthesis of SWNTs with controllable electronic type is of importance since they avoid difficult post-synthetic separation procedures. Most of the reported methods are based on the recombination of carbon atoms from a carbon feed source with the aid of catalyst nanoparticles, a proper choice of the catalyst particles and carbon source providing ways to control the growth of SWNTs.

SWNTs have been selectively grown with a high percentage of (6,5) and (7,5) semiconducting SWNTs from Co/Mo catalysts (CoMoCat)[22]. Li *et al.*[7] and Qu *et al.*[23] have reported selective growth of semiconducting nanotubes using plasma-enhanced chemical vapor deposition (CVD). High-density arrays of horizontally aligned SWNTs consisting of over 95% semiconducting nanotubes were obtained on single crystal quartz substrates by Ding *et al.*[5] He *et al.*[24] have used a magnesia (MgO)-supported iron-copper (FeCu) catalyst to accomplish the growth of predominantly (6, 5) SWNTs using carbon monoxide as the carbon source at ambient pressure. Chiang *et al.*[25] have obtained desired chiral SWNTs by varying the composition of the Ni_xFe_{1-x} nanocatalyst (Fig. 4). Li *et al.*[26] report bimetallic FeRu catalyst to obtain SWNTs with a narrow diameter and chirality distribution. At 600 °C, methane CVD on the FeRu catalyst produced predominantly (6,5) SWNTs. At 850 °C, the dominant semiconducting species were (8,4), (7,6), and (7,5) SWNTs, with narrower diameter distributions. They were further able to enrich (8,4) tubes by ion exchange chromatography. Ghorannevis *et al.*[27]

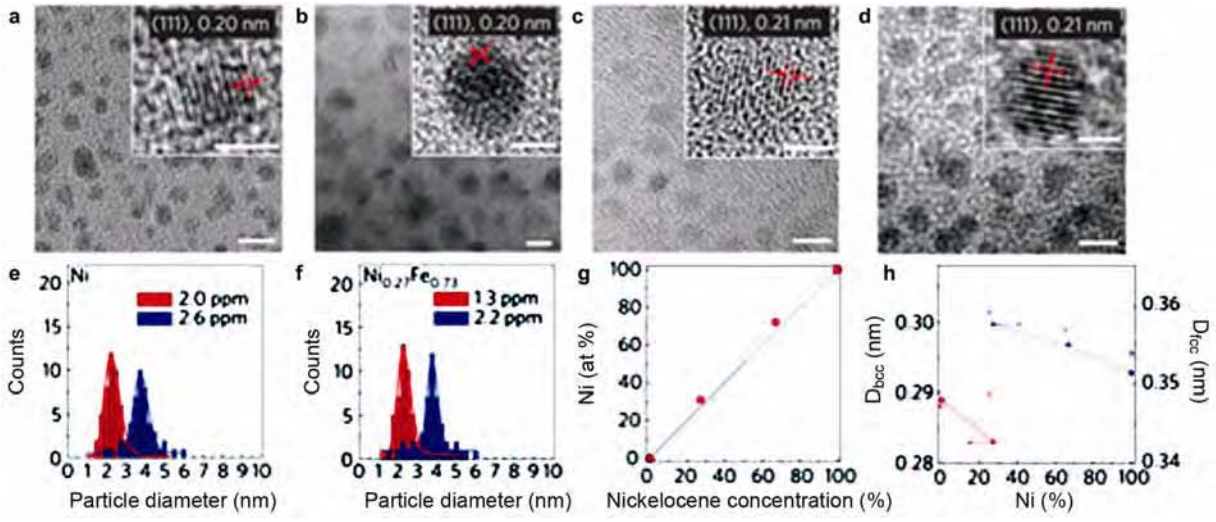

Fig. 4 — TEM images of Ni particles grown in a microplasma reactor at (a) 2.0 ppm and (b) 2.6 ppm nickelocene vapour concentration in Ar (scale bar: 5 nm). TEM images of $Ni_{0.27}Fe_{0.73}$ particles grown in a microplasma reactor at (c) 1.3 ppm and (d) 2.2 ppm total metallocene vapour concentration (27:73 nickelocene:ferrocene) (scale bar: 5 nm). Histograms of (e) Ni and (f) $Ni_{0.27}Fe_{0.73}$ particle diameters assessed from corresponding low-magnification TEM images. (g) EDX analysis of as-grown Ni_xFe_{1-x} nanoparticles. (h) XRD analysis of as-grown Ni_xFe_{1-x} nanoparticles. [Reproduced from Ref. 25 with permission from Nature Publishing Group, London, UK].

have demonstrated nonmagnetic (i. e. Au) catalyzed synthesis of narrow-chirality distributed SWNTs by plasma-enhanced CVD and have shown that hydrogen concentration plays a critical role in achieving narrow chirality distribution.

Hong *et al.*[10] report a simple way to directly grow semiconducting SWNT arrays with the assistance of ultraviolet (UV) irradiation (Fig. 5). This was done by introducing UV beam in the CVD system. They believe that the selection process took place at the very beginning of the SWNT formation rather than destroying the metallic SWNTs after growth. Ding *et al.*[5] report high-density arrays of perfectly aligned SWNTs consisting almost exclusively of semiconducting nanotubes grown on single crystal quartz substrates and propose that introducing methanol in the growth process as well as with the interaction between the SWNTs and the quartz lattice lead to selective growth of aligned semiconducting nanotubes.

Dai *et al.*[23] have attained the preferential synthesis of vertically aligned SWNTs with the percentage content of semiconducting nanotubes up to 96% by a combined use of plasma-enhanced CVD and fast heating for the pyrolysis of C_2H_2 at low pressures (~ 30 mTorr). The selective growth of bulk SWNT samples enriched with three different dominant chiralities including (6,5), (7,5), and (7,6) nanotubes becomes possible by adjusting the pressure of carbon monoxide on Co-Mo catalysts[28] from 2 to 18 bar. It is possible to tune the proportion of each type of chiral nanotube by changing the pressure of carbon monoxide.

Synthesis of Metallic SWNTs

There are very few reports on the selective synthesis of metallic SWNTs. A method for the synthesis of pure or nearly pure metallic SWNTs is highly desirable. Enriched metallic SWNTs (up to 65%) seem to be produced by the pyrolysis of monohydroxy alcohols[29]. Harutyunyan *et al.*[4] were able to obtain a fraction of nanotubes with metallic conductivity from one-third of the population to a maximum of 91% by varying the noble gas ambient during thermal annealing of the Fe nanocatalysts deposited on a SiO_2/Si support. *In situ* transmission electron microscope studies reveal that this variation leads to differences in both morphology and coarsening behavior of the nanoparticles used to

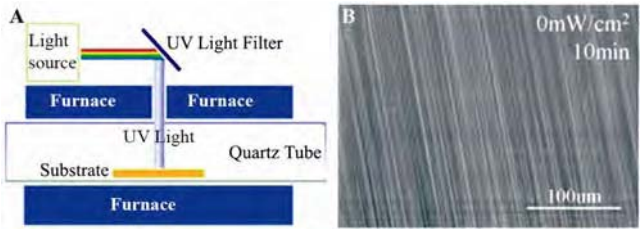

Fig. 5 — (A) Sketch map of the chemical vapor deposition system. (B) SEM image of SWNTs produced on quartz substrate. [Reproduced from Ref. 10 with permission from American Chemical Society, Washington DC, USA].

nucleate nanotubes. It would therefore appear that there is a relation between catalyst morphology and the resulting nanotube electronic structure, indicating that chiral-selective growth may indeed be possible (Fig. 6).

A systematic study of the effect of iron pentacarbonyl ($Fe(CO)_5$) vapor on the nature of SWNTs produced in the arc-discharge process has been carried out[3,30,31]. Carrying out arc-discharge of the graphite rods (with the $Ni+Y_2O_3$ catalyst) in the presence of $Fe(CO)_5$ yields nanotube deposits on the walls of the discharge chamber, primarily containing $\geq$ 90% metallic SWNTs. The procedure is simple and provides a useful method to prepare metallic SWNTs. The sample prepared in the absence of $Fe(CO)_5$ shows three bands in the visible-near IR region, a band centered around 750 nm corresponding to the metallic nanotubes (M_{11}) and two bands around 1040 nm (S_{22}) and 1880 nm (S_{11}) due to the semiconducting (Fig. 7a). Optical absorption spectra from samples prepared in the presence of $Fe(CO)_5$ mainly show the band due to metallic species (M_{11}). The intensity of the M_{11} band increases with the flow rate of $Fe(CO)_5$ (Fig. 7b). From the integrated areas of the bands due to the metallic and the semiconducting species, the percentage of the metallic species is estimated to be to be 94% in the presence of $Fe(CO)_5$. Figure 8 shows the variation of the Raman G and RBM bands of the SWNTs (from web region) obtained at different flow rates of $Fe(CO)_5$. The metallic feature in the Raman G-band increases with the increase in the $Fe(CO)_5$ flow rate. Different catalyst combinations have been studied to elucidate the role of $Fe(CO)_5$ in the formation of metallic nanotubes. Table 1 gives a summary of the various catalysts used. Only the $Ni+Y_2O_3$ catalyst under an optimal flow of $Fe(CO)_5$ yields metallic SWNTs.

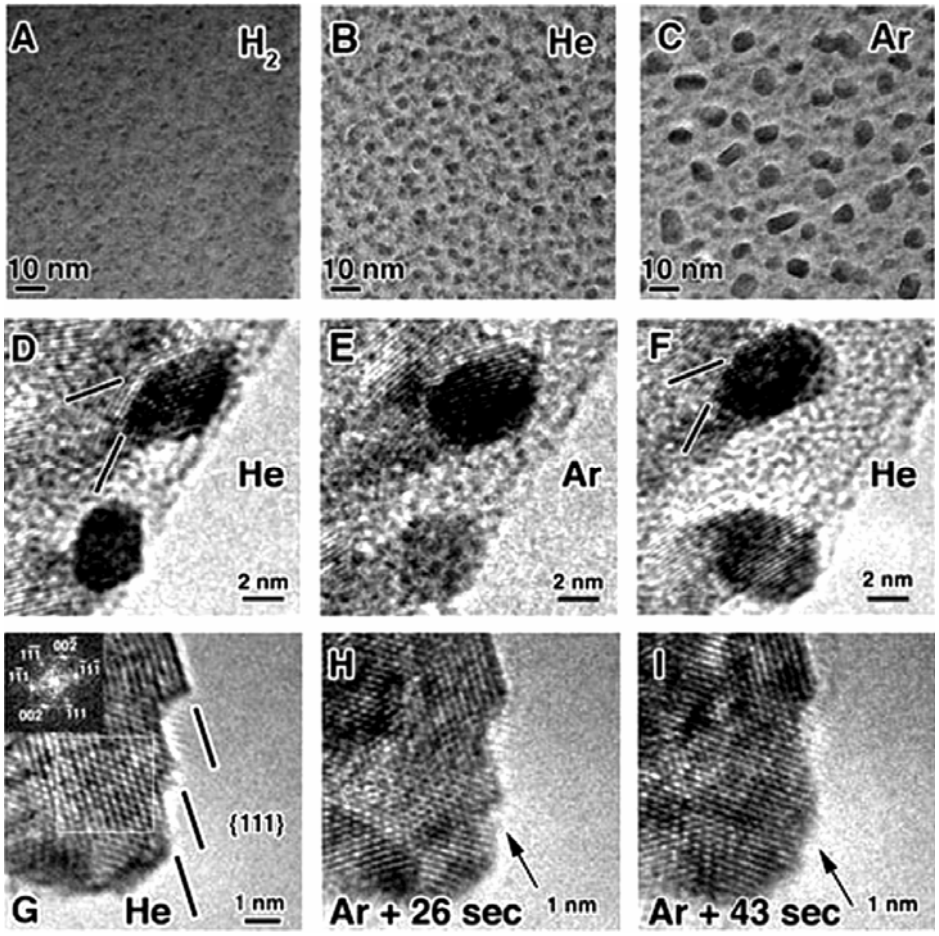

Fig. 6 — High-resolution transmission electron micrographs of Fe catalyst as a function of gas environment. (A to C) Size evolution of Fe catalysts after 60 min under (A) H_2, (B) He and (C) Ar at 500 °C and 500 mTorr. (D to F) Series of images from the same two Fe catalyst particles held at 500 °C, as the gas overpressure is changed from (D) 500 mTorr He to (E) 500 mTorr Ar to (F) 500 mTorr He. (G to I) Series of images from a larger Fe catalyst particle along a 110 zone axis. (G) Image taken in 500 mTorr He at 500 °C, showing very strong {111} facets. The inset diffractogram confirms the zone axis orientation. (H) After the introduction of Ar, local degradation of the facets begins. (I) With further time at 500 °C in the Ar environment, the facet has been completely removed. For all cases, the H_2O with base pressure of 10–2 mTorr is present. Arrows in (H) and (I) indicate the gradual defaceting features over time. [Reproduced from Ref. 4 with permission from AAAS. http://www.sciencemag.org, USA].

Post-synthetic Separation Methods

Methods to separate metallic and semiconducting SWNTs include dielectrophoresis, ultracentrifugation, selective destruction of one type of nanotubes by irradiation or by chemical means, selective interaction with molecules and covalent or noncovalent functionalization.

Non-covalent interactions

By making use of the selective interaction of aliphatic amines with functionalized SWNTs, separation of metallic and semiconducting SWNTs has been demonstrated[32-34]. Preferential charge-transfer interaction of bromine with the metallic species in surfactant-stabilized SWNTs, followed by centrifugation, has been used to separate semiconducting from metallic SWNTs[35]. Derivatized porphyrins selectively interact with semiconducting SWNTs through noncovalent interaction[36]. Such interaction can be employed to obtain semiconducting species in solution, leaving the metallic species as residue. Ozawa *et al.*[37] have designed fluorine-based copolymers for the recognition/extraction of specific (n, m) chiral SWNTs. The chiral copolymers were prepared by the Ni^0-catalyzed Yamamoto coupling reaction of 2,7-dibromo-9,9-di-n-decylfluorene and 2,7-dibromo-9,9-bis[(S)-(fl)-2-methylbutyl]fluorine co-monomers. The selectivity of the SWNT chirality is determined by the relative fraction of the achiral and chiral side groups. Chen *et al.*[38] separated

high purity (7,5) nanotubes by fluorene-based polymer wrapping process from SWNTs produced by using the Co-MCM-41 catalyst. The fluorene-based polymers are able to selectively wrap the SWNTs with certain chiral angles or diameters depending on their chemical structures. Poly(9,9-dioctyfluoreny1-2, 7-diyl) and poly[(9,9-dihexylfluorenyl-2,7-diyl)-co-(9,10-anthracene)] selectively wrap the SWNTs with high chiral angles (>24.5°) whereas poly[9,9-dioctylfluorenyl-2,7-diyl)-co-1,4-benzo-{2,1-3}-thiadiazole)] preferentially wraps the SWNTs with certain diameter (1.02-1.06 nm). Adsorption of specifically designed and geometrically constrained polyaromatic amphiphiles on SWNTs is selective with respect to the nanotube helicity angle with pentacenic-based amphiphiles leading to the solubilization of armchair SWNTs and quaterrylene-based amphiphile leading to the solubilization of zigzag SWNTs [39].

Zheng *et al.*[16,40-42] have designed short DNA sequences for the separation of SWNTs based on chirality. They were successful in separating 12 major single-chirality semiconducting species from a synthetic mixture by a 20 short DNA sequences which were preselected from a DNA library of 10^{60} in size using chromatographic purification (Fig. 9). The selectivity is based on the fact that recognition sequences exhibit a periodic purine-pyrimidines pattern, which undergoes hydrogen bonding to selectively form a two dimensional sheet, fold on the nanotubes and generate a well-ordered three-dimensional barrel. The ordered 2D sheet and 3D barrel appear to

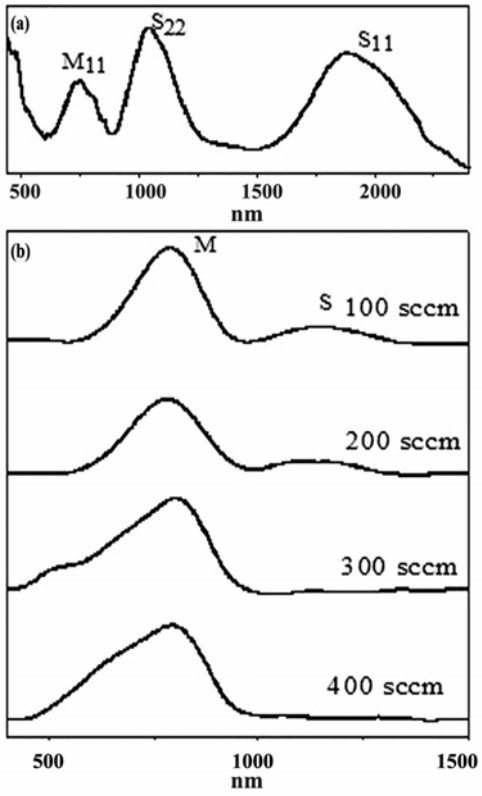

Fig. 7 — Optical absorption spectra of SWNTs samples (collected from the web region) (a) obtained with Ni+ Y_2O_3 catalyst alone and (b) with Ni+ Y_2O_3 in the presence of $Fe(CO)_5$. [Reproduced from Ref. 31].

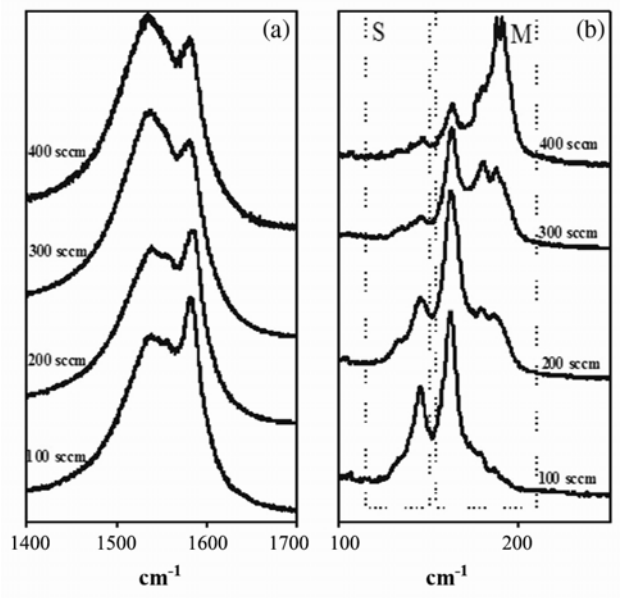

Fig. 8 — (a) G and (b) RBM bands in the Raman spectra of SWNTs obtained at different flow-rates of $Fe(CO)_5$. [Reproduced from Ref. 31].

Table 1 — SWNT formation with various catalysts in different atmospheres

Catalyst			With $Fe(CO)_5$		With CO	
	Cathode	Web	Cathode	Web	Cathode	Web
Ni + Y_2O_3	Metallic + Semi	Metallic + Semi	Metallic + Semi	Metallic	Metallic + Semi	Metallic + Semi
Ni	Not formed	Not formed	Not formed	Not formed	Not formed	Not formed
Fe	Not formed	Not formed	Not formed	Not formed	Not formed	Not formed
Ni + Fe	Not formed	Metallic + Semi	Not formed	Metallic + Semi	Not formed	Metallic + Semi

provide the structural basis for the DNA recognition of SWNTs. Ju *et al.*[43] report a method where the higher affinity of the flavin mononucleotide assembly for (8,6)-SWNTs results in an 85% chirality enrichment from a nanotube sample with broad diameter distribution. Cooperative hydrogen bonding between adjacent flavin moieties results in the formation of a helical ribbon, which organizes around SWNTs through π–π interactions between the flavin mononucleotide and the underlying graphene wall. Semiconducting SWNTs are extracted using DNA block copolymers

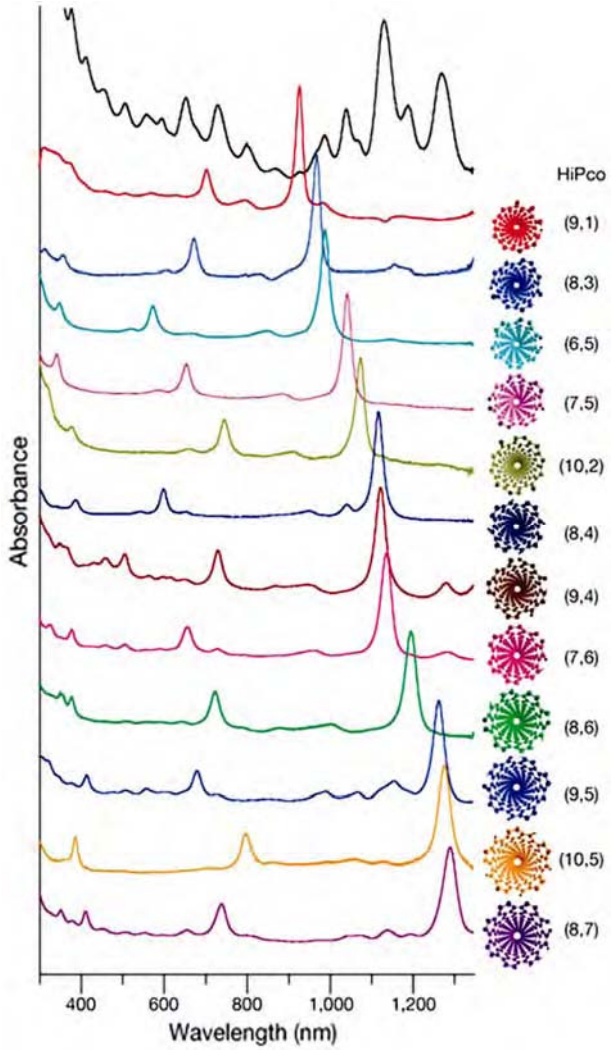

Fig. 9 — Optical absorption spectra of 12 purified semiconducting SWNTs (ranked according to the measured E_{11} absorption wavelength) and the starting HiPco mixture. The structure of each purified SWNT species (viewed along the tube axis) and its (n,m) notation are given at the right side of the corresponding spectrum. [Reproduced from Ref. 40 with permission from Nature Publishing Group, London, UK].

(DBC; poly(9,9-di-*n*-octylfluorenyl-2,7-diyl) covalently connected to 22-mer single-stranded (ss) oligo-deoxynucleotides multifunctional self-assembled micelles[44]. The hydrophobic polymer segments interact with the SWNT sidewall, enabling the dispersion of particular semiconducting nanotube species whereas the free DNA is utilized for facile hybridization with targets in solution and site-specific immobilization onto surfaces. Specific chiral nanotubes can be extracted from HiPco and CoMoCat SWNTs using salmon genomic DNA (SaDNA) and $d(GT)_{20}$. Genomic DNA specifically enriches (6,5) SWNTs as compared to (10,3) tubes whereas $d(GT)_{20}$ shows little or no chirality preference[45].

Peng *et al.*[46] have obtained optically active SWNTs through preferential extraction of metallic (m)- or semiconducting (s)-SWNTs with 2,6-pyridylene-bridged chiral diporphyrins. In the circular dichroism (CD) spectra, SWNTs extracted with 2,6-pyridylene-bridged chiral diporphyrins exhibit much larger intensity than those with 1,3-phenylene-bridged chiral diporphyrins, indicating chiral discrimination ability of the former diporphyrins. (6,5)-SWNTs display the most intensified CD signals among the SWNTs extracted with 2,6-pyridylene-bridged chiral diporphyrins. The improved discrimination and extraction abilities of 2,6-pyridylene-bridged chiral diporphyrins are attributed to the formation of more stable SWNT complex. Optically active SWNT samples are obtained by preferentially extracting either right- or left-handed SWNTs from a commercial sample. Chiral gabletype porphyrin molecules bind with different affinities to the left- and right-handed helical nanotube isomers to form complexes with different stabilities. The diporphyrins can be removed from the complexes to provide optically enriched SWNTs[47].

Molecular charge-transfer between SWNTs and an appropriate π-system has been exploited for the effective separation of metallic and semiconducting nanotubes, since π-π interaction with aromatic molecules enables the solubilization of SWNTs, exhibiting selectivity in the interaction of electron-donor and -acceptor molecules with SWNTs[48]. The potassium salt of coronene tetracarboxylic acid, which has a large π skeleton attached to four electron-withdrawing groups, is found to exhibit charge-transfer interaction with SWNTs[49]. The

interaction causes precipitation of metallic nanotubes due to greater affinity of the electron withdrawing molecule to metallic SWNTs. Thus, the separation occurs due to molecular charge-transfer between coronene tetracarboxylate and SWNTs, and is accompanied by the debundling of the SWNTs. The solubilization of semiconducting SWNTs in water can be attributed to the weak interaction with coronene salt. The separation process is therefore simple and involves sonication followed by the precipitation of the metallic nanotubes. The solution contains only the semiconducting nanotubes (Fig. 10). The simplicity of the method allows bulk separation of SWNTs, giving 100 % separation with the appropriate concentration of potassium salt of coronene tetracarboxylate. Noncovalent interaction of derivatized pyrenes has been used for the separation of metallic and semiconducting SWNTs.[50] Feng *et al.*[51] carried out non-covalent polymer sorting of SWNTs by using polyvinylpyrrolidone (PVP) in dimethylformamide (DMF). With long-term standing of SWNTs/PVP/DMF in ambient condition, the semiconducting SWNTs remain suspended in the solvent while the metallic SWNTs precipitate out. These authors propose that non-covalent charge-transfer occurs between PVP and SWNTs, and that the metallic nanotubes with mobile electrons at/near the Fermi level are more susceptible to environmental temperature fluctuations than semiconducting nanotubes. The small temperature increase experienced during 14 days of standing under normal laboratory conditions, causes the unwrapping of the polymer from the metallic nanotubes, leading to selective precipitation.

Hong *et al.*[52] have employed scotch tape technique for separation of metallic (m) and semiconducting (s) SWNTs analogous to the popular method used for peeling graphite into atomically thin graphene layers. They have chosen soft polydimethylsiloxane (PDMS) thin films as the supporting material, while 3-aminopropyl-triethoxysilane ($C_9H_{23}NO_3Si$, APTES, defined as A-scotch tape) and triethoxyphenylsilane ($C_{12}H_{20}O_3Si$, PTEOS, defined as P-scotch tape) were used as the bonding material to introduce amine and phenyl functional groups respectively. When the PDMS-based scotch tape is applied to a mixture of m- and s-SWNTs, A-scotch tape selectively removes s-SWNTs, while the P-scotch tape adheres to the metallic ones.

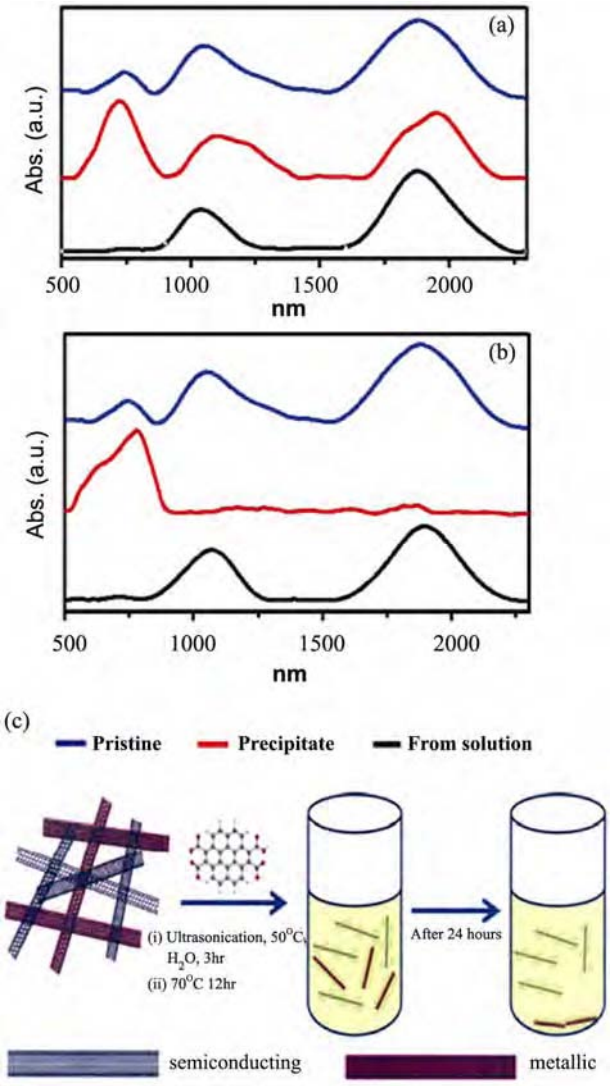

Fig. 10 — Optical absorption spectra of pristine SWNTs (1, blue), precipitate (2, red) and SWNTs from solution (3, black) obtained with (a) 5 m*M* and (b) 10 m*M* of coronene salt. (c) Schematic depicting the separation of SWNTs. [Reproduced from Ref. 49 with permission from American Chemical Society, Washington DC, USA].

Covalent chemistry

Smalley *et al.*[53] employed diazonium reagents for the selective functionalization of metallic nanotubes with near exclusion of semiconducting nanotubes under controlled conditions. Thus, hydroxybenzene -diazonium salt selectively functionalizes metallic SWNT. Subsequent deprotonation in alkaline solution followed by electrophoretic separation results in the enrichment of the metallic and semiconducting fractions separately[45,47]. Ghosh and Rao[30,54] carried out the enrichment of metallic SWNTs using fluorous chemistry[30,54]. Here, the

diazonium salt of 4-heptadecafluorooctylaniline was made to selectively react with the metallic nanotubes present in the mixture and SWNTs functionalized by the fluorous tag were extracted using a fluorous hydrocarbon (Fig. 11). Fluorous chemistry is a fine method available today for purification (with nearly 100% efficiency) as it involves merely attaching a fluorous tag to a substrate and then extracting the tagged moiety into a fluorous solvent. The extent of separation of the metallic nanotubes can be evidenced by the spectroscopic measurements. Figure 11(b) shows the optical absorption spectra of the fluorous extract and precipitate. The fluorous extract shows optical bands corresponding to m-SWNTs. On the other hand, the precipitate shows s-SWNT, demonstrating that the fluorous extract almost entirely consists of metallic SWNTs. The purity of the separated metallic SWNTs was estimated to be nearly 95%.

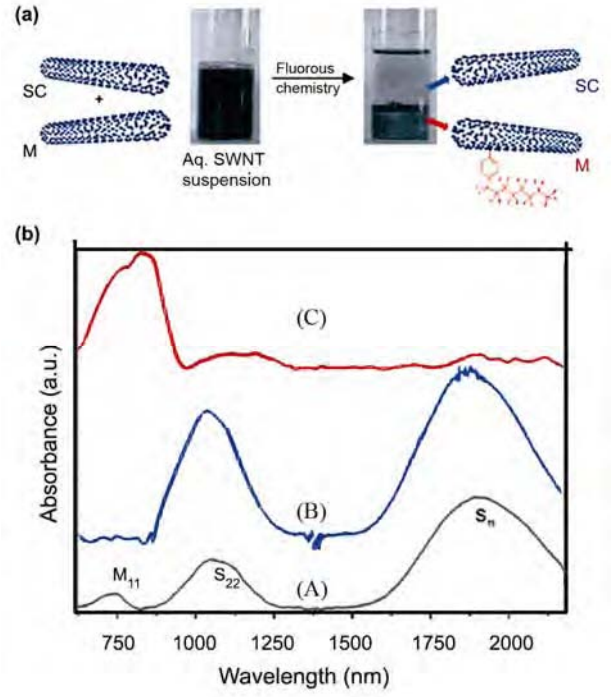

Fig. 11 — (a) Schematic of the reaction with a diazonium salt followed by fluorous extraction enables separation of semiconducting (upper aqueous layer) and metallic single walled carbon nanotubes (lower fluorous layer). (b) Electronic absorption spectra of (A) as-prepared pure SWNTs; (B) residue left in the aqueous layer after the fluorous extraction and annealing at 600 °C; (C) solid obtained from the fluorous extract after removal of the diazonium functionality by heating at 600 °C. [Reproduced from Ref. 54 with permission from Springer-Verlag, Berlin, Germany].

Cycloaddition of fluorinated olefins is used as an effective approach toward converting as-grown SWNT mats into high-mobility semiconducting tubes with high yield, without any further need for separation processing[55]. Microwave-assisted treatment of as-received HiPco SWNTs suspended in mixed acids has been used as a means for enriching s-SWNTs through preferential elimination of m-SWNTs. This procedure also been employed for diameter-dependent sorting and diameter-distribution narrowing[56].

Dielectrophoresis

Making use of the differences in the relative dielectric constants of semiconducting and metallic species with respect to the solvent, alternating current dielectrophoresis has been employed to separate the two species[57]. In this procedure, the SWNT suspension is dropped on the microelectrode array. The metallic tubes which acquire the largest dipole moments migrate towards the electrodes, while the semiconducting tubes remain in suspension during this process. Shin *et al.*[58] have developed a microfluidic channel with two inlets and two outlets for the separation of semiconducting and metallic SWNTs by dielectrophoresis (Fig. 12).

Density gradient ultracentrifugation

Density gradient ultracentrifugation (DGU) is a useful method for the separation of SWNTs. DGU separates materials based on the subtle variations in their buoyant density. It is a commonly used method to separate and isolate proteins and poly(nucleic acids). In this method, the mixture is loaded into an aqueous solution with a known density gradient. The centripetal force of an ultracentrifuge makes the species migrate toward their respective isopycnic points, where their density matches that of the gradient. With a suitable choice of the initial gradient, the species are spatially separated by density. Arnold *et al.*[59] applied the DGU method to enrich DNA-wrapped SWNTs in aqueous density gradients (aqueous dilutions of iodixanol were used as density gradient media) based on the diameter of the nanotubes. Separation is radially identified by the formation of colored bands of SWNTs in the density range of 1.11-1.17 g cm^{-3}. SWNTs with decreasing diameter are found to be increasingly more buoyant. A hydrodynamic model, which empirically

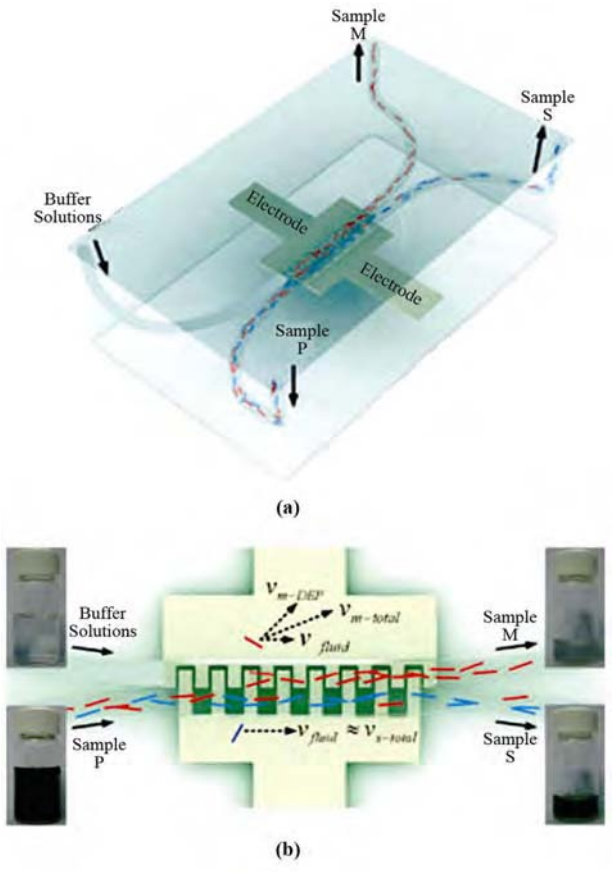

Fig. 12 — Schematic of the experimental setup. (a) An H-shaped channel with two inlets and two outlets is shown. The labels M and S designate samples of pure metallic and enriched semiconducting SWNTs collected at each outlet. (b) The separation mechanism based on dielectrophoresis is shown. Metallic SWNTs (red rods) were subjected to a significantly larger dielectrophoretic force, perpendicular to the direction of the flow, than semiconducting SWNTs (blue rods). [Reproduced from Ref. 58 with permission from American Chemical Society, Washington DC, USA].

incorporates a diameter dependence of the surfactant monolayer packing density, has been used to describe this order.[60] Due to the limited stability of DNA wrapped nanotubes in aqueous solution, Arnold *et al.*[11] showed that bile salts and their mixtures with other surfactants enable the separation of SWNTs by diameter, band gap and/or electronic type. Isolation of specific chirality SWNTs can be refined by carrying out the separation in multiple successive density gradients. The adsorption of surfactants to SWNTs is reversible and the method is compatible with a wide range of tube diameters (0.7–1.6 nm) (Fig. 13). When using co-surfactant mixtures of sodium cholate and SDS, electronic-type sorting by DGU is achieved. The latter sorting was attributed to inequivalent binding of the two surfactants as a function of the SWNT polarizability, which produced differences in the density of the SWNT–surfactant hybrid depending on the electronic nature of SWNTs. Antaris *et al.*[61] used nonionic, biocompatible block copolymers to isolate semiconducting and metallic SWNTs using DGU. These workers show that Pluronics with shorter hydrophobic chain lengths leads to higher purity semiconducting SWNTs, whereas X-shaped tetronic block copolymers display an affinity for metallic SWNTs. Bonaccorso *et al.*[62] analyzed the performance of different surfactants such as bile salts (e.g. sodium cholate, sodium deoxycholate, and sodium taurodeoxycholate) which are more effective in individualizing SWNTs than linear chain surfactants (e.g. sodium dodecylbenzene sulfonate and SDS) for use in DGU. Haroz *et al.*[63] obtained samples enriched in metallic SWNTs by DGU employing a three-surfactant system. Use of the chiral surfactant, sodium cholate, results in enantiomer separation, which discriminates between left- and right-handed SWNTs, thereby inducing subtle differences in their buoyant densities. This sorting strategy has been employed for simultaneous enrichment by the handedness and the roll-up vector of SWNTs[64] in the diameter range of 0.7 to 1.5 nm. Nonlinear DGU has been applied to separate different semiconducting nanotubes from SWNTs samples produced by the HiPco process[65].

Chromatography

Chromatography is one of the most commonly used methods for separation of organic compounds. Few groups have attempted to separate SWNTs through column chromatography wherein one type of SWNTs has a stronger affinity with the stationary phase than the other. Surfactant-wrapped SWNTs tend to bind onto a stationary phase such as silica gel tightly making it hard to elute them from the column. Tanaka *et al.*[66] have developed an electrophoresis method using a column filled with agarose gel to separate SWNTs. When SWNTs embedded in agarose gel were eluted with SDS solution, only metallic SWNTs separated from the starting gel in an electric field, giving rise to two separate fractions. Based on the selective adsorption of agarose gel, a gel-squeezing method has been developed to separate SWNTs[15]. Under

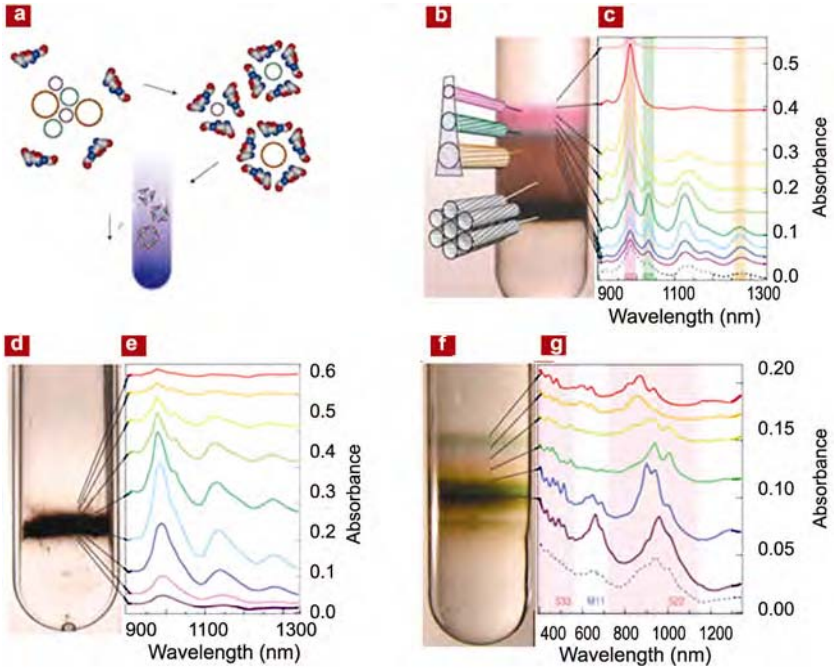

Fig. 13 — (a) Schematic of surfactant encapsulation and sorting, where rho is density. (b–g) Photographs and optical absorbance (1 cm path length) spectra after separation using density gradient ultracentrifugation. [Reproduced from Ref. 11 with permission from Nature Publishing Group, London, UK].

the squeezing action, metallic nanotubes are released into the solution phase whilst semiconducting nanotubes remain in the agarose gel matrix. A continuous method using a column has been developed to facilitate scaling-up of the separation process in which the s-SWNTs were tightly bound to the gel and were not eluted when the column was washed with 1% SDS solution, whereas the m-SWNTs were eluted. Subsequent elution with 1% sodium deoxycholate solution results in the release of the bound s-SWNTs as a gel-free solution fraction[67] (Fig. 14). It was found that agarose gel as the medium for gel column chromatography required the use of a surfactant solution with a high dispensability to elute the bound s-SWNTs and that diameter dependent resolution is poor at high concentration of sodium deoxycholate. Moshammer *et al.*[68] successfully separated m- and s-SWNTs using an allyl dextran-based size-exclusion gel.

Liu *et al.*[69] have developed a single-surfactant multicolumn gel chromatography in which several gel columns are connected vertically in series to achieve large-scale chirality separation using ally dextran-based size exclusion gel as stationary phase and SDS as a mobile phase (Fig. 15). The method involves loading an excess amount of SWNT

Fig. 14 — Separation of SWNTs by a gel-squeezing method in which a piece of gel containing SWNTs and SDS was frozen, thawed and squeezed. [Reproduced from Ref. 15 with permission from American Chemical Society, Washington DC, USA].

dispersion in a SDS aqueous solution onto the top column, giving rise to selective adsorption of s-SWNTs with different chiralities in the various columns on the basis of the strengths of their interactions with the gel. Metallic SWNTs exhibit the lowest interaction with the gel and are collected as unbound nanotubes. These workers are able to separate 13 major (n, m) species from a HiPco grown nanotubes by performing a second separation of each s-SWNT fraction. In this chromatography strategy, it is necessary to find an effective stationary or mobile phase with different affinities towards the different types of SWNTs. By a suitable choice of stationary and mobile phases, chromatography allows easy and scalable separation, which can be used on industrial scale.

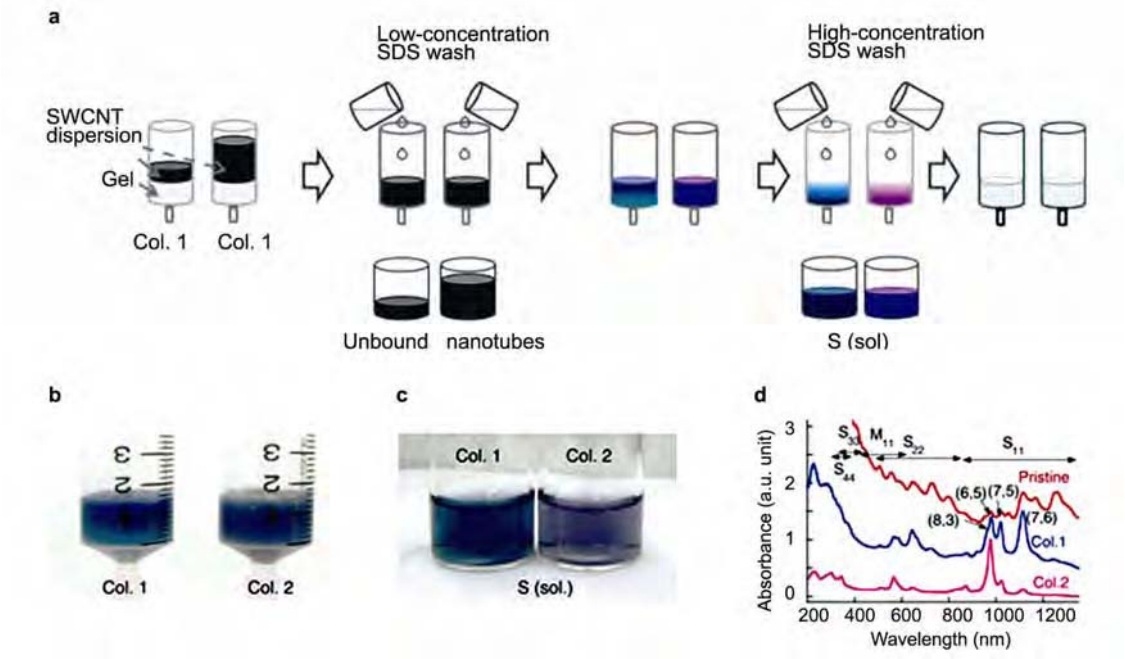

Fig. 15 — (a) Schematic diagram of overloading effect with SWNTs in the gel columns. 1- and 8-ml aliquots of SWNT dispersion were loaded into Col. 1 and Col. 2, respectively. (b) Photograph of the gel columns after washing the unbound nanotubes. (c) Photograph of the collected s-SWNT solutions from Cols. 1 (left) and 2 (right). (d) Optical absorption spectra of nanotubes selectively adsorbed in the gel columns. The spectrum for the HiPco (pristine) SWNTs was measured as a reference. The blue shaded region (200–300 nm) in (d) indicates the ultraviolet optical absorption characteristic of the nanotubes. (Col., column; S, semiconducting; sol., solution). [Reproduced from Ref. 69 with permission from Nature Publishing Group, London, UK].

Y-junction SWNTs

Synthesis of junction carbon nanotubes has been an important challenge. There have been efforts to create junction multi-walled carbon nanotubes by using template methods[70]. To obtain large yields of branched CNTs, the most used route is to introduce additives such as thiophene in the reactants, which was first reported in 2000 by Satish kumar *et al.*[71] MWNT junctions were produced by the pyrolysis of nickelocene (which acts both as the catalyst source and the carbon feedstock) in the presence of thiophene. A similar CVD process with different additives has been employed to generate branched MWNTs.[72] The role of sulfur (thiophene) in the branching process of nanotubes with stacked-cone morphologies has been explained[73]. The growing branches appear to possess a minute amount of sulfur, which is sufficient to promote the formation of heptagons (negative curvature) and pentagons (positive curvature).

Multi-terminal SWNTs have interesting electronic properties compared to Y-junction SWNTs. Y-junction SWNTs were seen in STM samples produced by the thermal decomposition of C_{60} in the presence of transition metals like Ti, Cr, Fe, Co and Ni[74]. Choi and coworkers[75] synthesized Y-junction SWNTs using thermal CVD of methane over Mo or Zr doped Fe nanoparticles supported on aluminum oxide. The presence of Mo or Zr in the Fe catalyst enhances the nucleation and growth of carbon nanotubes and facilitates the growth of new nanotube branches when they are attached to the sidewalls of the existing nanotubes.

A procedure to synthesize Y-junction SWNTs by arc-discharge method has been described. Y-junction SWNTs have been obtained by the arc-evaporation of graphite rods (filled Ni and Y_2O_3) in thiophene and He atmosphere[31] (660 Torr). The SWNTs can be purified by acid and hydrogen treatment. Figure 16 shows TEM images of Y-junction SWNTs obtained by this method. The TEM images show that the diameter of arms in Y-junction SWNTs varies between 1.6 and 2 nm. Figure 17 shows the AFM image of the Y-junction

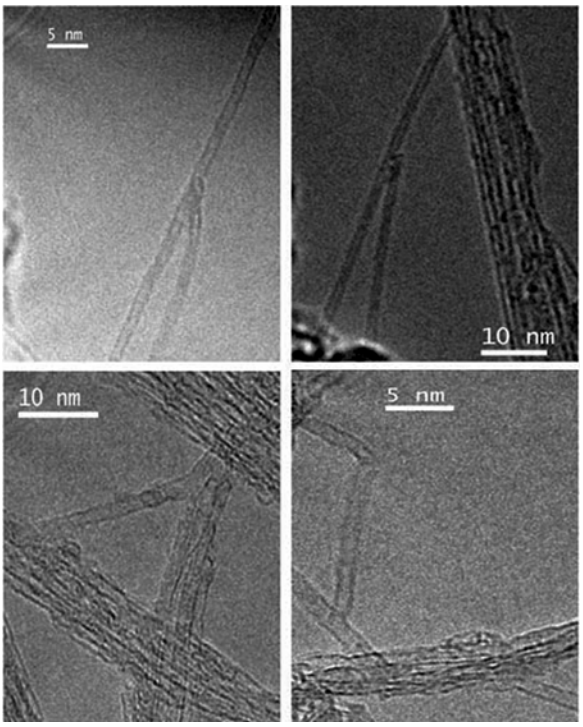

Fig. 16 — TEM images of Y-junction single-walled carbon nanotubes. [Reproduced from Ref. 31].

SWNTs. Junction SWNTs are occasionally observed during conventional synthetic processes. Multiterminal SWNTs have been found in the thermal CVD process using Mo or Zr-doped Fe nanoparticles supported by aluminum oxide particles. Here, junction growth is attributed to the excess nucleation by Mo or Zr. The mechanism of junction formation using thiophene is different and the presence of sulfur plays a key role in the branching mechanism. One does not observe the junctions in the absence of sulfur. Recent theoretical calculations suggest that sulfur energetically favors pentagonal rings and heptagonal rings over hexagons, thereby introducing negative curvatures (heptagons, branch opening) or positive curvatures (pentagons, closing its tip)[76]. Sulfur is likely to induce the appearance of a bud along the structure and to promote the formation of junctions. It should be noted that the electronic properties of the junction are unique. Thus, the junction may exhibit transistor characteristics.

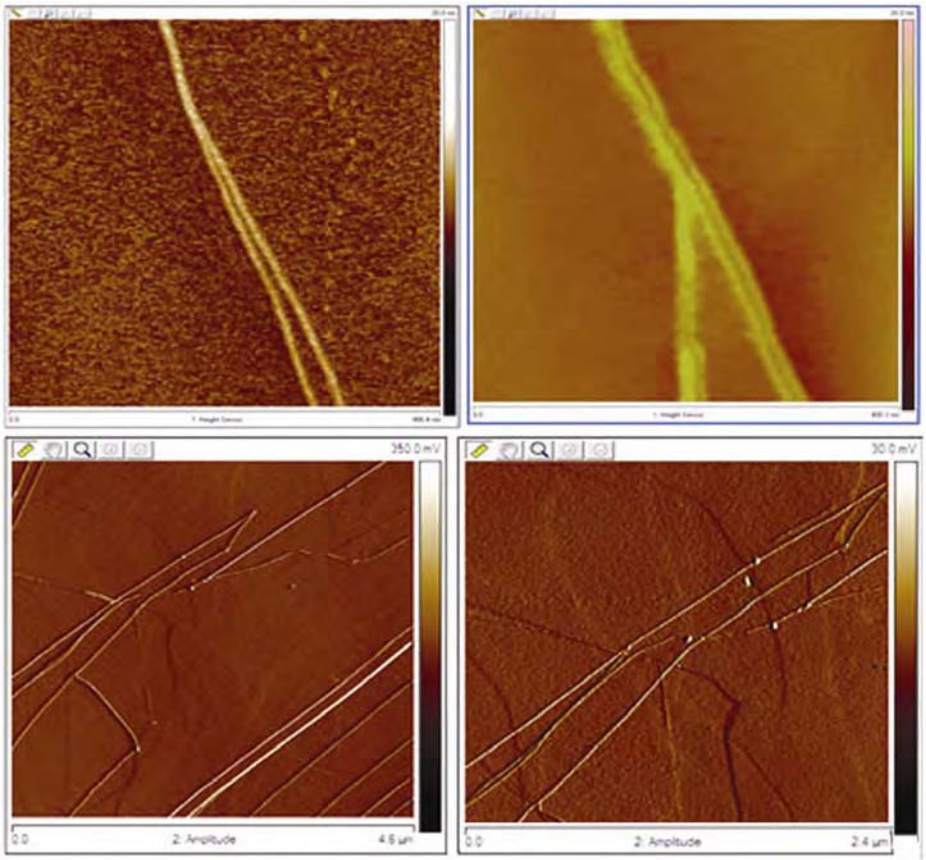

Fig. 17 — AFM images of Y-junction SWNTs. [Reproduced from Ref. 31].

Concluding Remarks

The previous sections describe the present status of various methods to generate pure metallic and semiconducting SWNTs either by direct synthesis or by separation of mixtures. Clearly, the problem has not been entirely solved. We are yet to discover a simple and straightforward procedure to synthesize semiconducting or metallic SWNTs in pure form. There is still scope for research in developing efficient separation protocols for SWNTs which can be used readily. We require methods to produce pure metallic and semiconducting nanotubes with specific chirality on a large scale.

References

1 Rao C N R & Govindaraj A, *Nanotubes and Nanowires*, Secon Edition (RSC Nanoscience & Nanotechnology series, Royal Society of Chemistry, Cambridge, UK) 2011.

2 Dresselhaus M S, Dresselhaus G & Eklund P C, *Science of Fullerenes and Carbon Nanotubes*, (Academic Press, San Diego, USA) 1996.

3 Rao C N R, Voggu R & Govindaraj A, *Nanoscale*, 1 (2009) 96.

4 Harutyunyan A R, Chen G, Paronyan T M, Pigos E M, Kuznetsov O A, Hewaparakrama K, Kim S M, Zakharov D, Stach E A & Sumanasekera G U, *Science*, 326 (2009) 116.

5 Ding L, Tselev A, Wang J, Yuan D, Chu H, McNicholas T P, Li Y & Liu J, *Nano Lett*, 9 (2009) 800.

6 Bachilo S M, Balzano L, Herrera J E, Pompeo F, Resasco D E & Weisman R B, *J Am Chem Soc*, 125 (2003) 11186.

7 Li Y, Mann D, Rolandi M, Kim W, Ural A, Hung S, Javey A, Cao J, Wang D, Yenilmez E, Wang Q, Gibbons J F, Nishi Y & Dai H, *Nano Lett*, 4 (2004) 317.

8 Kato T & Hatakeyama R, *ACS Nano*, 4 (2010) 7395.

9 Wenseleers W, Vlasov I I, Goovaerts E, Obraztsova E D, Lobach A S & Bouwen A, *Adv Funct Mater*, 14 (2004) 1105.

10 Hong G, Zhang B, Peng B, Zhang J, Choi W M, Choi J-Y, Kim J M & Liu Z, *J Am Chem Soc*, 131 (2009) 14642.

11 Arnold M S, Green A A, Hulvat J F, Stupp S I & Hersam M C, *Nature Nanotechnol*, 1 (2006) 60.

12 S. Duesberg G, Burghard M, Muster J & Philipp G, *Chem Commun*, (1998) 435.

13 Hersam M C, *Nature Nanotechnol*, 3 (2008) 387.

14 Miyata Y, Maniwa Y & Kataura H, *J Phys Chem B*, 110 (2005) 25.

15 Tanaka T, Jin H, Miyata Y, Fujii S, Suga H, Naitoh Y, Minari T, Miyadera T, Tsukagoshi K & Kataura H, *Nano Lett*, 9 (2009) 1497.

16 Zheng M, Jagota A, Semke E D, Diner B A, McLean R S, Lustig S R, Richardson R E & Tassi N G, *Nature Mater*, 2 (2003) 338.

17 Roberts M E, LeMieux M C, Sokolov A N & Bao Z, *Nano Lett*, 9 (2009) 2526.

18 Dresselhaus M S, Dresselhaus G & Jorio A, *J Phys Chem C*, 111 (2007) 17887.

19 Dresselhaus M S, Dresselhaus G, Jorio A, Souza Filho A G & Saito R, *Carbon*, 40 (2002) 2043.

20 Ouyang M, Huang J-L & Lieber C M, *Acc Chem Res*, 35 (2002) 1018.

21 Hamon M A, Itkis M E, Niyogi S, Alvaraez T, Kuper C, Menon M & Haddon R C, *J Am Chem Soc*, 123 (2001) 11292.

22 Wang B, Poa C H P, Wei L, Li L-J, Yang Y & Chen Y, *J Am Chem Soc*, 129 (2007) 9014.

23 Qu L, Du F & Dai L, *Nano Lett*, 8 (2008) 2682.

24 He M, Chernov A I, Fedotov P V, Obraztsova E D, Sainio J, Rikkinen E, Jiang H, Zhu Z, Tian Y, Kauppinen E I, Niemela M & Krause A O I, *J Am Chem Soc*, 132 (2010) 13994.

25 Chiang W-H & Mohan Sankaran R, *Nature Mater*, 8 (2009) 882.

26 Li X, Tu X, Zaric S, Welsher K, Seo W S, Zhao W & Dai H, *J Am Chem Soc*, 129 (2007) 15770.

27 Ghorannevis Z, Kato T, Kaneko T & Hatakeyama R, *J Am Chem Soc*, 132 (2010) 9570.

28 Wang B, Wei L, Yao L, Li L-J, Yang Y & Chen Y, *J Phys Chem C*, 111 (2007) 14612.

29 Wang Y, Liu Y, Li X, Cao L, Wei D, Zhang H, Shi D, Yu G, Kajiura H & Li Y, *Small*, 3 (2007) 1486.

30 Voggu R, Ghosh S, Govindaraj A & Rao C N R, *J Nanosci Nanotechnol*, 10 (2010) 4102.

31 Voggu R, *Investigations of New Methods of Synthesis, Phenomena and Novel Properties of Nanocarbons and Other Nanomaterials*, Ph D Thesis, JNCASR, Bangalore, 2010.

32 Chattopadhyay D, Galeska I & Papadimitrakopoulos F, *J Am Chem Soc*, 125 (2003) 3370.

33 Ju S-Y, Utz M & Papadimitrakopoulos F, *J Am Chem Soc*, 131 (2009) 6775.

34 Maeda Y, Kanda M, Hashimoto M, Hasegawa T, Kimura S-I, Lian Y, Wakahara T, Akasaka T, Kazaoui S, Minami N, Okazaki T, Hayamizu Y, Hata K, Lu J & Nagase S, *J Am Chem Soc*, 128 (2006) 12239.

35 Chen Z, Du X, Du M-H, Rancken C D, Cheng H-P & Rinzler A G, *Nano Lett*, 3 (2003) 1245.

36 Li H, Zhou B, Lin Y, Gu L, Wang W, Fernando K A S, Kumar S, Allard L F & Sun Y-P, *J Am Chem Soc*, 126 (2004) 1014.

37 Ozawa H, Fujigaya T, Niidome Y, Hotta N, Fujiki M & Nakashima N, *J Am Chem Soc*, 133 (2011) 2651.

38 Chen F, Wang B, Chen Y & Li L-J, *Nano Lett*, 7 (2007) 3013.

39 Marquis R, Greco C, Sadokierska I, Lebedkin S, Kappes M M, Michel T, Alvarez L, Sauvajol J-L, Meunier S & Mioskowski C, *Nano Lett*, 8 (2008) 1830.

40 Tu X, Manohar S, Jagota A & Zheng M, *Nature*, 460 (2009) 250.

41 Zheng M, Jagota A, Strano M S, Santos A P, Barone P, Chou S G, Diner B A, Dresselhaus M S, Mclean R S, Onoa G B, Samsonidze G G, Semke E D, Usrey M & Walls D J, *Science*, 302 (2003) 1545.

42 Zheng M & Semke E D, *J Am Chem Soc*, 129 (2007) 6084.

43 Ju S-Y, Doll J, Sharma I & Papadimitrakopoulos F, *Nature Nanotechnol*, 3 (2008) 356.

44 Kwak M, Gao J, Prusty D K, Musser A J, Markov V A, Tombros N, Stuart M C A, Browne W R, Boekema E J, ten Brinke G, Jonkman H T, van Wees B J, Loi M A & Herrmann A, *Angew Chem Int Ed*, 50 (2011) 3206.

45 Kim S N, Kuang Z, Grote J G, Farmer B L & Naik R R, *Nano Lett*, 8 (2008) 4415.

46 Peng X, Komatsu N, Kimura T & Osuka A, *J Am Chem Soc*, 129 (2007) 15947.

47 Peng X, Komatsu N, Bhattacharya S, Shimawaki T, Aonuma S, Kimura T & Osuka A, *Nature Nanotechnol*, 2 (2007) 361.
48 Varghese N, Ghosh A, Voggu R, Ghosh S & Rao C N R, *J Phys Chem C*, 113 (2009) 16855.
49 Voggu R, Rao K V, George S J & Rao C N R, *J Am Chem Soc*, 132 (2010) 5560.
50 Anilkumar P, Fernando K A S, Cao L, Lu F, Yang F, Song W, Sahu S, Qian H, Thorne T J, Anderson A & Sun Y-P, *J Phys Chem C*, 115 (2011) 11010-15.
51 Feng J, Alam S M, Yan L Y, Li C M, Judeh Z, Chen Y, Li L-J, Lim K H & Chan-Park M B, *J Phys Chem C*, 115 (2011) 5199.
52 Hong G, Zhou M, Zhang R, Hou S, Choi W, Woo Y S, Choi J-Y, Liu Z & Zhang J, *Angew Chem Int Ed*, 50 (2011) 6819.
53 Strano M S, Dyke C A, Usrey M L, Barone P W, Allen M J, Shan H, Kittrell C, Hauge R H, Tour J M & Smalley R E, *Science*, 301 (2003) 1519.
54 Ghosh S & Rao C N R, *Nano Res*, 2 (2009) 183.
55 Kanungo M, Lu H, Malliaras G G & Blanchet G B, *Science*, 323 (2009) 234.
56 Qiu H, Maeda Y & Akasaka T, *J Am Chem Soc*, 131 (2009) 16529.
57 Krupke R, Hennrich F, Lohneysen H v & Kappes M M, *Science*, 301 (2003) 344.
58 Shin D H, Kim J-E, Shim H C, Song J-W, Yoon J-H, Kim J, Jeong S, Kang J, Baik S & Han C-S, *Nano Lett*, 8 (2008) 4380.
59 Arnold M S, Stupp S I & Hersam M C, *Nano Lett*, 5 (2005) 713.
60 Nair N, Kim W-J, Braatz R D & Strano M S, *Langmuir*, 24 (2008) 1790.
61 Antaris A L, Seo J-W T, Green A A & Hersam M C, *ACS Nano*, 4 (2010) 4725.
62 Bonaccorso F, Hasan T, Tan P H, Sciascia C, Privitera G, Di Marco G, Gucciardi P G & Ferrari A C, *J Phys Chem C*, 114 (2010) 17267.
63 Haroz E H, Rice W D, Lu B Y, Ghosh S, Hauge R H, Weisman R B, Doorn S K & Kono J, *ACS Nano*, 4 (2010) 1955.
64 Green A, Duch M & Hersam M, *Nano Res*, 2 (2009) 69.
65 Ghosh S, Bachilo S M & Weisman R B, *Nature Nanotechnol*, 5 (2010) 443.
66 Tanaka T, Jin H, Miyata Y & Kataura H, *App Phys Express*, 1 (2008) 114001.
67 Tanaka T, Urabe Y, Nishide D & Kataura H, *App Phys Express*, 2 (2009) 125002.
68 Moshammer K, Hennrich F & Kappes M, *Nano Res*, 2 (2009) 599.
69 Liu H, Nishide D, Tanaka T & Kataura H, *Nature Commun*, 2 (2011) 309.
70 Li J, Papadopoulos C & Xu J, *Nature*, 402 (1999) 253.
71 Satishkumar B C, Thomas P J, Govindaraj A & Rao C N R, *App Phys Lett*, 77 (2000) 2530.
72 Deepak F L, Govindaraj A & Rao C N R, *Chem Phys Lett*, 345 (2001) 5.
73 Romo-Herrera J M, Sumpter B G, Cullen D A, Terrones H, Cruz-Silva E, Smith D J, Meunier V & Terrones M, *Angew Chem Int Ed*, 47 (2008) 2948.
74 Terrones M, Banhart F, Grobert N, Charlier J C, Terrones H & Ajayan P M, *Phys Rev Lett*, 89 (2002) 075505.
75 Kim D-H, Huang J, Shin H-K, Roy S & Choi W, *Nano Lett*, 6 (2006) 2821.
76 Romo-Herrera J M, Cullen D, A, Cruz-Silva E, Ramírez D, Bobby G S, Meunier V, Humberto T, David J S & Mauricio T, *Adv Funct Mater*, 19 (2009) 1193.